

Wind Field Estimation from UAV Data using Machine Learning

Vijay Shankar Dwivedi¹, Hyo-Sang Shin², and Antonios Tsourdos³

¹ Cranfield University, Cranfield, Bedfordshire MK400AL, UK,
VijayShankar.Dwivedi@cranfield.ac.uk

² Professor, Cranfield University, Cranfield, Bedfordshire MK400AL, UK,
h.shin@cranfield.ac.uk

Professor, KAIST, Cho Chun Shik Graduate School of Mobility, 34141, Daejeon,
Republic of Korea, hyosangshin@kaist.ac.kr

³ Professor, Cranfield University, Cranfield, Bedfordshire MK400AL, UK,
a.tsourdos@cranfield.ac.uk

Abstract. Wind data is critical for aircraft safe operation and air traffic management. Especially during the transition and reverse transitions of vertical takeoff and landing UAVs dynamic information of wind-field is vital. This paper proposes a 1-D convolutional neural network-based dynamic estimation of the wind-field for a UAV. Simulation is carried out for the generation of trim input data for different wind and trim conditions which is based on analytical approach. Nonlinear constrained optimization is performed to determine trim input. Further, the set of control inputs and trim states are used to train and validate the proposed neural network.

Nomenclature

(u, v, w) : components of aircraft translational velocity relative to earth-fixed frame in aircraft body axes X_b , Y_b and Z_b respectively

$(\dot{u}, \dot{v}, \dot{w})$: components of aircraft translational acceleration in aircraft body frame

(p, q, r) : components of aircraft rotational velocities in the aircraft body frame (roll, pitch and yaw rates respectively)

$(\dot{p}, \dot{q}, \dot{r})$: components of aircraft rotational acceleration in aircraft body frame

(F_x, F_y, F_z) : components of total forces acting on aircraft in the body frame

$(F_{A_{x_b}}, F_{A_{y_b}}, F_{A_{z_b}})$: components of aerodynamic forces acting on aircraft in the body frame

$(F_{g_{x_b}}, F_{g_{y_b}}, F_{g_{z_b}})$: components of gravitational forces acting on aircraft in the body frame

(ϕ, θ, ψ) : roll pitch and yaw angles respectively

$(\dot{\phi}, \dot{\theta}, \dot{\psi})$: roll pitch and yaw rates respectively

m : aircraft mass

g : gravitational acceleration

D, Y, L : drag, side force, and lift force respectively

C_D, C_Y, C_L : coefficients of drag, side force, and lift respectively

$C_{D_0}, C_{Y_0}, C_{L_0}$: coefficients of drag, side force, and lift respectively
 $(\Gamma_1, \Gamma_2, \Gamma_3, \Gamma_4, \Gamma_5, \Gamma_6)$: Intermediate coefficients
 (I_{xx}, I_{yy}, I_{zz}) : moment of inertia about roll axis, pitch axis and yaw axis respectively
 I_{xz} : product of inertia
 α : angle of attack
 β : sideslip angle
 γ : flight path angle
 $(\dot{\alpha}, \dot{\beta}, \dot{\gamma})$: rates of α, β and γ respectively
 R_{WB} : transformation matrix from wind to body frame
 R_ϕ, R_θ : transformation matrix from Euler rotations ϕ and θ respectively
 ρ : air density
 S : aircraft wing area
 T : thrust force
 V : true air speed
 W_n, W_e, W_d : components of wind-field in NED frame
 V_{trim} : trim speed
 γ_{trim} : trim flight path angle
 C : cost function
 W : weight matrix
 b : bias vector
 η : learning rate
 Θ : network parameter matrix
 n : length of dataset
Subscripts
 E : elevator
 A : aileron
 R : rudder
 T : throttle
 Aux : auxiron
 min : minimum deflection limit
 max : maximum deflection limit

1 Introduction

The wind field is an important parameter for flight mission planning. For an aircraft to operate within the flight envelope, information about wind field is required. Aircraft performance parameters and operations are determined by the presence of wind [1]. Conventionally flight routes are planned to utilize the wind fields for improving fuel economy [2] [3]. Landing and takeoff operations are planned based on the presence of wind. A tailwind increases runway requirements while a headwind decreases takeoff and landing distances. A crosswind also limits the safety of takeoff and landing. Apart from UAV operations, wind estimate is required for different atmospheric sampling applications [4].

For tasks like optimum path planning, safety assessment, etc., prior information on the wind field is desired. Whereas in modern aviation there are certain areas where dynamic information on wind is required. Detect and avoid operation is an example where dynamic information of wind is required [5], as the direction of wind alters the maneuverability in different directions of the UAV and therefore wind information is critical for detect and avoid algorithms. A smooth and safe transition is desired for VTOL UAVs from multi-rotor to fixed-wing or fixed-wing to multi-rotor modes. In order to achieve such a transition, it is essential to align the UAV with the wind direction and hence wind field estimate is required. For efficient execution of the above studies, real-time estimation of the wind field is essential.

Several methods have been developed for estimating wind fields. Space-based Doppler lidar system is a widely used method for generating wind data [6]. Some modern aircraft are equipped with Doppler radar, which can detect wind speed and direction by measuring the frequency shift of radio waves reflected off moving objects such as raindrops or dust particles [7]. These are most widely used methods in modern aviation and are suitable for large aircraft, for small to medium UAVs these equipment are not suitable due to their weight and cost. Ground-based weather observations based methods are also used in manned aviation where meteorological agencies provide weather reports that include wind speed and direction at various altitudes. Pilots can use this information to estimate the wind during flight. This is also not suitable for small UAVs, as this requires an additional communication link and access to this service provider. Inertial navigation system along with GPS and pitot measurement is also used to estimate wind speed and direction. The INS and GPS measures the aircraft's ground speed and heading and compares it to the airspeed and heading. The difference between the two can be used to calculate the wind speed and direction [8]. Based on this approach several studies have been done to estimate real-time wind fields. In [9], the wind is estimated using ground speed from GPS and relative wind speed from pitot measurements. A model based estimation is proposed in [10]. Wind estimation for a tail sitter aircraft is done in [11], and data from the pitot tube is fused with an extended Kalman filter. A post-flight wind estimation method is proposed in [12]. With these methods, additional sensor inputs are required and due to the involvement of system dynamics, the computational cost is high. In recent years data-driven methods have gained popularity due to their simplicity and ability to extract useful information from data. A multi-objective optimization algorithm is proposed in [13] that uses identification errors to propose the wind-speed components. An H-infinity filtering approach with test flight results for a fixed wing aircraft is used for estimating wind in [14].

The real-time estimation of the wind field is critical for UAVs. There are sophisticated methods where aircraft dynamics is involved. This becomes even more complex when information from additional sensors like GPS and pitot is involved. In the era of machine learning and data science, data-driven deep learning techniques can be used to estimate the wind field with lesser computational cost and minimal sensor information.

In a flight the relationship between control inputs and outputs (flight states) is influenced by the presence of the wind. Hence extracting information of wind field from flight data of inputs and outputs in real time should be possible. This paper aims to develop a wind estimation algorithm based on the input and output data. Note that the information of aircraft states are readily available with flight control and navigational units. Also, control inputs are available with flight control unit which generates pulse width modulated (PWM) signals to command actuators.

During a flight, the influence of the wind is always present on the flight states and thus at any moment of the time wind field can be estimated. However, considering wind estimation during all the maneuvers can be less effective. Whenever the rate variables are associated with the flight maneuver, it requires real-time estimation of several states that depend on the past values which adds uncertainty and measurement error. Also, the more number of states is, the more computational effort is required. To make computation simpler and reliable, we suggest to the wind estimation during trim phase where rate variables are zero. The flight data stream is continuously observed and trim is identified. Values associated with trim state are used for estimating wind.

An aircraft flying at a particular trajectory and speed corresponds a particular trim state. To achieve this trim, a set of control inputs is required. The presence of a wind-field alters the flight condition and for the aircraft to maintain the same trajectory a new trim state is required and hence a new set of control inputs. It is trivial that the new trim state and control inputs have information about wind-field within itself which is extracted in the work presented in this paper. Data-driven approach for real-time wind estimation is an essential contribution of this work.

This research article proposes real-time estimation of wind field based on aircraft states and control input required for achieving a particular trim by designing a multivariate 1-D convolutional neural network. The rationale behind using neural networks for wind estimation in aircraft is that they are able to learn complex patterns and relationships between input and output data, which may be difficult to model using traditional methods or too complex to compute. Further, there are several logical reasons why neural networks are a suitable approach for wind estimation in aircraft. Traditional mathematical techniques can struggle to model non-linear relationships between inputs and outputs. However, neural networks are inherently non-linear, allowing them to capture complex relationships between the inputs (control inputs and flight states) and the output (wind-field). This is especially important when dealing with ever-changing wind patterns encountered during flight. Neural networks are able to learn and adapt to new data, making them well-suited for handling the wide range of conditions encountered during flight. As the aircraft encounters new wind patterns, the neural network can learn from this data and adjust its predictions accordingly. This adaptability makes neural networks a powerful tool for improving the accuracy of wind estimation. Neural networks are also able to generalize from a limited set of training data to make predictions on new data. This means that

even if the neural network has not encountered a particular wind pattern before, it can still make accurate predictions based on its understanding of the underlying relationships between the inputs and outputs. This generalization ability is essential for ensuring that the wind estimation system works reliably in a variety of different flight conditions. Modern neural networks can be trained and run on powerful computer hardware, allowing them to make predictions quickly and efficiently. This speed is essential for providing real-time wind estimation to aircraft, which is required for safer operation. Overall, the combination of non-linear modeling, adaptability, generalization, accuracy, real-time update, efficiency and speed makes neural networks a highly effective approach for wind estimation in aircraft.

The rest of the paper is composed as follows: UAV research platform is in section 2 where effect of the wind is analysed on a UAV and trim inputs are determined for a trim flight in the presence of wind. Proposed multi-variable regression-based wind estimation in section 3. Results, discussion and analysis is presented in section 4 and conclusions are given in section 5.

2 UAV Research Platform

Implementation of methodology proposed in this paper requires values of states during a trim. A trim is identified by looking at angular and linear rate variables that are available with navigational unit and its available with all the commercially available autopilots therefore no additional hardware is required for this. Once the trim flight is identified, variables required to estimate the wind-field is also already available with aircraft navigational unit. A process diagram for the methodology is shown in the Fig. (1)

For training and validating a neural network a large dataset is required containing a wide range of possible input conditions. Generating this dataset with practical flight tests is not feasible because this will need a wide range of possible wind conditions during the flight test which is unrealistic. Therefore, the dataset is generated using a simulation platform where a wide range of wind conditions along with aircraft trim is achieved more conveniently. Further, to develop a simulation platform, the parameters of a real UAV are required. Parameters of UAV Maraal are used as a test case for simulation[15].

2.1 Simulation Platform

To generate data set for training the neural network and validating it, simulation is carried out in a MATLAB environment. As the objective of this study is to estimate the wind field during a straight trim flight using UAV control inputs and trim conditions, it is required to develop an analytical model of UAV dynamics that includes wind conditions. Further, a method is required to trim the UAV at different flight paths and wind conditions. The behavior of a UAV for wind conditions and control inputs depends on the UAV dynamics and its parameters and this is investigated in the following subsection.

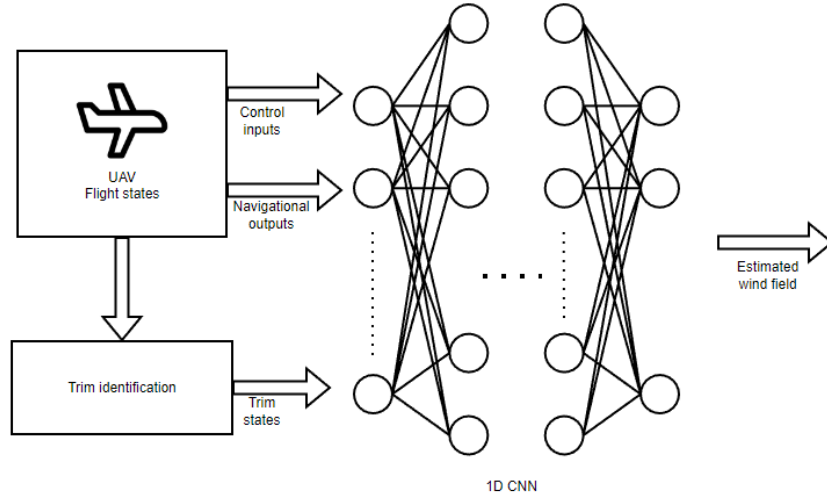


Fig. 1. Process of wind-field estimation in a UAV using 1-D CNN

2.2 UAV Dynamics

In order to develop aircraft equations of motion, standard equations of motion are modified and the wind is incorporated into them. The standard governing equations for the motion of a UAV are given in Eqs. (1) to (9) which are defined in an inertial reference frame.

$$\dot{u} = rv - qw + \frac{F_x}{m} \quad (1)$$

$$\dot{v} = pw - ru + \frac{F_y}{m} \quad (2)$$

$$\dot{w} = qu - pv + \frac{F_z}{m} \quad (3)$$

$$\dot{p} = \Gamma_1 pq - \Gamma_2 qr + \Gamma_3 l + \Gamma_4 n \quad (4)$$

$$\dot{q} = \frac{1}{I_{yy}} (M - pr(I_{xx} - I_{zz}) - I_{xz}(p^2 - r^2)) \quad (5)$$

$$\dot{r} = \Gamma_5 pq - \Gamma_1 qr + \Gamma_4 l + \Gamma_6 n \quad (6)$$

$$\dot{\phi} = p + q \sin(\phi) \tan(\theta) + r \cos(\phi) \tan(\theta) \quad (7)$$

$$\dot{\theta} = q \cos(\phi) - r \sin(\phi) \quad (8)$$

$$\dot{\psi} = q \sin(\phi) \sec(\theta) + r \cos(\phi) \sec(\theta) \quad (9)$$

$$(10)$$

Table 1. Inertia Parameters

$$\begin{array}{c}
 \Gamma_1 \frac{I_{xz}(I_{xx}-I_{yy}+I_{zz})}{I_{xx}I_{zz}-I_{xz}^2} \\
 \Gamma_2 \frac{I_{zz}(I_{zz}-I_{yy})+I_{xz}^2}{I_{xx}I_{zz}-I_{xz}^2} \\
 \Gamma_3 \frac{I_{zz}}{I_{xx}I_{zz}-I_{xz}^2} \\
 \Gamma_4 \frac{I_{xz}}{I_{xx}I_{zz}-I_{xz}^2} \\
 \Gamma_5 \frac{(I_{xx}-I_{yy})I_{xz}+I_{xz}^2}{I_{xx}I_{zz}-I_{xz}^2} \\
 \Gamma_6 \frac{I_{xx}}{I_{xx}I_{zz}-I_{xz}^2}
 \end{array}$$

where $\Gamma_1, \Gamma_2, \Gamma_3, \Gamma_4, \Gamma_5$ and Γ_6 are constants and given in Table 1. F_x, F_y and F_z are resultant of aerodynamic, thrust and gravitational forces acting in aircraft body X-axis, Y-axis and Z-axis respectively.

Components of the aerodynamic forces acting on the aircraft in the aircraft body frame are given by

$$\begin{bmatrix} F_{A_{x_b}} \\ F_{A_{y_b}} \\ F_{A_{z_b}} \end{bmatrix} = R_{BW} \begin{bmatrix} -D \\ Y \\ -L \end{bmatrix} = \begin{bmatrix} L \sin \alpha - D \cos \alpha \cos \beta - Y \cos \alpha \sin \beta \\ -D \sin \beta + Y \cos \beta \\ -D \sin \alpha \cos \beta - Y \sin \alpha \sin \beta - L \cos \alpha \end{bmatrix} \quad (11)$$

where, L, D and Y are lift, drag and Y-force acting on the aircraft respectively, R_{BW} is the transformation matrix from the wind frame to the body frame defined as

$$R_{BW} = \begin{bmatrix} \cos \alpha \cos \beta & -\cos \alpha \sin \beta & -\sin \alpha \\ \sin \beta & \cos \beta & 0 \\ \sin \alpha \cos \beta & -\sin \alpha \sin \beta & \cos \alpha \end{bmatrix} \quad (12)$$

For a roll angle, ϕ , and pitch angle, θ , components of gravitational forces $F_{g_{x_b}}, F_{g_{y_b}}$, and $F_{g_{z_b}}$ acting on the aircraft in the aircraft body frame are given by

$$\begin{bmatrix} F_{g_{x_b}} \\ F_{g_{y_b}} \\ F_{g_{z_b}} \end{bmatrix} = R_\phi R_\theta \begin{bmatrix} 0 \\ 0 \\ mg \end{bmatrix} \quad (13)$$

where, g is gravitational acceleration, R_ϕ and R_θ are transformation matrices for Euler rotations ϕ and θ respectively, defined as follows

$$R_\phi = \begin{bmatrix} 1 & 0 & 0 \\ 0 & \cos \phi & \sin \phi \\ 0 & -\sin \phi & \cos \phi \end{bmatrix} \quad (14)$$

$$R_\theta = \begin{bmatrix} \cos \theta & 0 & -\sin \theta \\ 0 & 1 & 0 \\ \sin \theta & 0 & \cos \theta \end{bmatrix} \quad (15)$$

Using Eqs. (11) and (13) for the components of the aerodynamic and gravitational forces acting on the aircraft in the aircraft body frame respectively, and considering, the thrust force (T) is aligned along the body X -axis. Net forces in the aircraft body frame F_x , F_y , and F_z are given by

$$\begin{bmatrix} F_x \\ F_y \\ F_z \end{bmatrix} = \begin{bmatrix} F_{A_{x_b}} + F_{g_{x_b}} + T \\ F_{A_{y_b}} + F_{g_{y_b}} \\ F_{A_{z_b}} + F_{g_{z_b}} \end{bmatrix} \quad (16)$$

Further, it is essential to incorporate the wind effect into the vehicle dynamics. Lift, drag, and Y-force used in Eq.11 are calculated using Eq.17

$$\begin{bmatrix} -D \\ Y \\ -L \end{bmatrix} = 0.5\rho V^2 S \begin{bmatrix} -C_D \\ C_Y \\ -C_L \end{bmatrix} \quad (17)$$

where, ρ is the density of air, S is wing area, C_D , C_Y , and C_L are coefficients of drag, side force, and lift respectively. V is true air speed and is given by Eq.18

$$V = [(u - W_n)^2 + (v - W_e)^2 + (w - W_d)^2]^{0.5} \quad (18)$$

where, u , v , and w are components of the velocity vector in the aircraft body frame and W_n , W_e , and W_d are components of the wind vector in NED frame in directions north, east, and down respectively.

Aerodynamic coefficients C_D , C_Y , and C_L are calculated using Eqs. 19- 21

$$C_L = C_{L_o} + C_{L_{\delta_E}} \delta_E + C_{L_\alpha} \alpha + C_{L_q} \frac{q\bar{c}}{2V} + C_{L_{\dot{\alpha}}} \frac{\dot{\alpha}\bar{c}}{2V} \quad (19)$$

$$C_D = C_{D_o} + kC_L^2 \quad (20)$$

$$C_Y = C_{Y_o} + C_{Y_{\delta_A}} \delta_A + C_{Y_{\delta_R}} \delta_R + C_{Y_\beta} \beta + C_{Y_p} \frac{pb}{2V} + C_{Y_r} \frac{rb}{2V} + C_{Y_{\dot{\beta}}} \frac{\dot{\beta}b}{2V} \quad (21)$$

where stability and control derivatives have their usual meaning. δ_E , δ_A and δ_R are elevator, aileron and rudder inputs respectively. α and β are angle of attack and sideslip angle respectively. p , q , r , $\dot{\alpha}$, and $\dot{\beta}$ are roll, pitch, yaw, angle of attack, and sideslip angle rates respectively. Values of α and β in the presence of wind are calculated using Eqs. 22 and 23. C_{D_o} is zero lift drag and k is given by Eq. (24).

$$\alpha = \tan^{-1} \frac{(w - W_d)}{(u - W_n)} \quad (22)$$

$$\beta = \sin^{-1} \frac{(v - W_e)}{V} \quad (23)$$

$$k = \frac{1}{\pi} ARc \quad (24)$$

where, AR is aspect ratio of aircraft wing and e is wing efficiency factor [16].

Further, to generate a dataset for training and validation of neural network it is required to determine control inputs for different trim conditions. In the next section, control inputs are determined to achieve a desired trim flight.

2.3 UAV Trim

The theoretical framework of the definition of trim is applied to the aircraft equations of motion. As the wind may come from any direction, it is important to consider the most generalized condition of equations of motion. Constrained minimization will work to find optimum values of elevator deflection δ_E , aileron deflection δ_A , rudder deflection δ_R , and throttle level δ_T .

To trim the UAV at flight speed V_{trim} and flight path angle γ_{trim} , the cost function (C) used for optimization is defined in Eq. 25

$$C = Q' H Q \quad (25)$$

where, H is an identity matrix of 11x11, and Q is defined as

$$Q = \left[\dot{u} \dot{v} \dot{w} p q r \dot{\alpha} \dot{\beta} (V - V_{trim}) (\gamma - \gamma_{trim}) \phi \right]' \quad (26)$$

Constraints for the optimization are given by

$$\begin{aligned} u &> 0 \\ \delta_{E_{min}} &\leq \delta_E \leq \delta_{E_{max}} \\ \delta_{A_{min}} &\leq \delta_A \leq \delta_{A_{max}} \\ \delta_{R_{min}} &\leq \delta_R \leq \delta_{R_{max}} \\ 0\% &\leq \delta_T \leq 100\% \end{aligned} \quad (27)$$

The objective of this study is to estimate the wind field during a flight using aircraft control inputs. For the development of 1-D CNN, components of the wind field W_n , W_e , and W_d are considered as output variables. Control inputs, elevator deflection (δ_E), aileron deflection (δ_A), rudder deflection (δ_R) and throttle percentage (δ_T) are used as input variables. Random values of aircraft speed in the range of $20m/s$ and $35m/s$, altitude ranging from $100m$ to $2000m$, and the flight path angle between $+10$ deg to -10 deg are used to generate the dataset which is used in the simulation framework for training the neural network in the next section.

3 Proposed Multi-variable Regression-based Wind Estimation

For estimating wind field a 1-D convolutional neural network-based deep network is designed for multivariate data.

3.1 Convolutional Neural Network

The original proposal of CNN [17] was for image recognition, as it has the capability to learn high-level representations from raw image data. When it comes to analyzing temporal data, a more principled approach is to use 1-D CNN [18]. Both 1-D and 2-D CNNs consist of input layers, hidden layers, dense layers, and an output layer. The computational cost of 1-D CNN is lower compared to 2-D CNN because it utilizes 1-D data for convolution. To update the trainable parameters of CNN, the back-propagation algorithm is employed, following the update rule described in (28), where \mathbf{W} represents the filter weight matrix, \mathbf{b} denotes the bias vector, and η represents the learning rate.

$$\mathbf{W} = \mathbf{W} - \eta \frac{\partial J(\mathbf{W}, \mathbf{b})}{\partial \mathbf{W}}, \quad \mathbf{b} = \mathbf{b} - \eta \frac{\partial J(\mathbf{W}, \mathbf{b})}{\partial \mathbf{b}} \quad (28)$$

Table 2. The resulting architecture of 1-D CNN.

Layer	Layer type	Filter size	filters	Strides	Padding	Activation function
1	convolutional	(8, 1)	32	1	No	ReLU
2	convolutional	(1,1)	32	4	No	ReLU
3	convolutional	(1,1)	64	4	No	ReLU
4	convolutional	(1,1)	64	4	No	ReLU
5	convolutional	(1,1)	128	4	No	ReLU
6	convolutional	(1,1)	128	4	No	ReLU
	flatten					
			Neurons			
7	dense		50			ReLU
8	dense		1			linear

3.2 Multivariate 1-D Convolutional Neural Network

The 1D CNN is a specialized variant of 2-D CNNs specifically designed to process time-series data. As depicted in Figure 2, the input to the 1-D CNN layer is a 2-D array with dimensions representing the input variable and time. The filters traverse along the time axis of the input variable to obtain channel outputs. To address wind-field estimation, Figure 3 showcases the designed 1-D CNN architecture. The inputs to the 1-D convolutional layer consist of elevator input (δ_E), aileron input (δ_A), rudder input (δ_R), throttle input (δ_T), airspeed (V), flight altitude (h), flight path angle (γ), and ground speed (u), each with n number of samples. These input variables are fed into the CNN layers with multiple kernels for feature extraction. Subsequently, the dense layers follow, where the first layer flattens the features from the r^{th} convolutional layer. In this designed architecture, Rectified Linear Unit (ReLU) is employed as the activation function for each layer except the output layer. The output layer (l^{th})

is linearly activated, meaning it is without non-linearity. The Mean Squared Error (MSE) is utilized as the cost function, as defined in (29), where y_i and \hat{y}_i represent the actual and predicted powers, respectively, and Θ denotes the network parameters matrix.

$$J(\Theta) = \frac{1}{n} \left[\sum_{i=1}^n (y_i - \hat{y}_i)^2 \right] \quad (29)$$

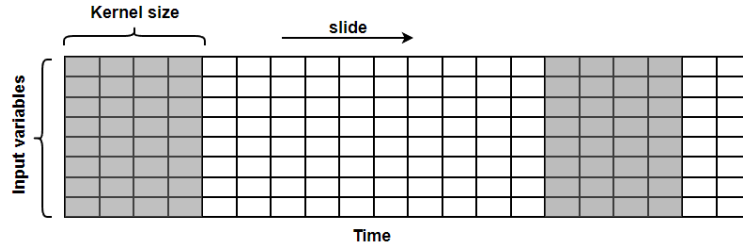


Fig. 2. 1-D CNN structure used for wind field estimation.

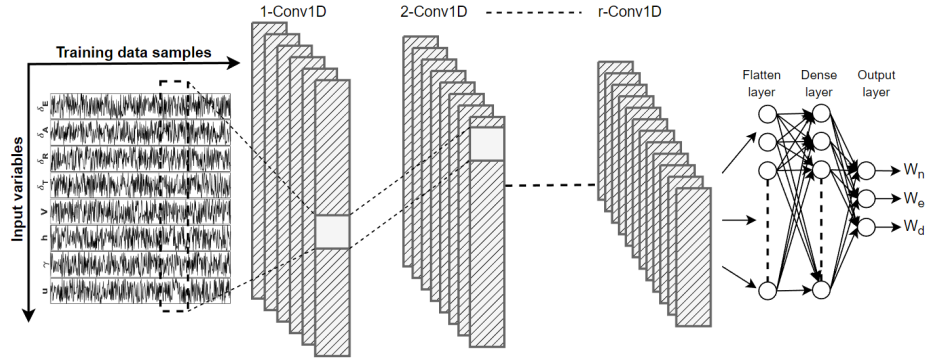


Fig. 3. Framework of wind-field estimation using 1-D CNN. The input variables are elevator input (δ_E), aileron input (δ_A), rudder input (δ_R), throttle input (δ_T), airspeed (V), flight altitude (h), flight path angle (γ), and ground speed (u).

4 Results, Discussion, and Analysis

An analytical model has been developed for the estimation of trim inputs for a given trim condition in the presence of wind field. Using this model a database

is generated for training and validating a neural network. The computations were executed on a computer equipped with an i7-12700 processor and 32 GB of RAM.

4.1 Evaluation Metrics

To evaluate the performance of the proposed methodology, we utilize Root Mean Square Error (RMSE) and Mean Absolute Error (MAE) as metrics. These metrics are defined in equations (30) and (31) respectively.

$$\text{RMSE} = \sqrt{\frac{1}{n} \left[\sum_{i=1}^n (y_i - \hat{y}_i)^2 \right]} \quad (30)$$

$$\text{MAE} = \frac{1}{n} \left[\sum_{i=1}^n |y_i - \hat{y}_i| \right] \quad (31)$$

where n represents the length of the test data. RMSE measures the change in the predicted value, while MAE provides a more accurate reflection of the predicted error. Smaller values of RMSE and MAE indicate better estimation performance.

4.2 Simulation Results

As mentioned earlier, a total of 25,000 samples were generated using an analytical method for training the network. These data samples were divided into a training set and a testing set, with the testing set comprising 15% of the total samples. During the network training process, 15% of the data set was utilized for validation purposes. Various architectures were explored in order to devise a lightweight and high-performing 1-D CNN architecture for wind-field estimation in flight missions. The architecture that yielded the best results in terms of performance and efficiency is presented in Table 2. The table provides details of the architecture, where "dense" denotes a fully connected layer, and "ReLU" refers to a rectified linear unit. The input shape of the network is set to 1×8 , where 8 corresponds to the number of input variables. The Adam optimizer is utilized for training the 1D-CNN network. During training, the number of epochs is set to 100, and the batch size is set to 50. Figure 4 illustrates the Mean Square Error (MSE) in relation to the number of epochs during the training process of the designed network. Table 3 presents the quantitative evaluation of the proposed method, demonstrating the RMSE and MAE results for random samples. Lower values of RMSE and MAE indicate more accurate estimation outcomes. This Table shows estimation results on randomly selected test dataset for winds from different directions. The visualization of the estimation results on the test data using the proposed method is depicted in Fig 5. To enhance visualization, the estimated results are magnified by focusing on smaller windows.

Table 3. RMSE and MAE for different wind components

Proposed method	RMSE	MAE
all components (random samples)	7.03	8.71
North	6.98	8.28
East	5.88	6.29
Down	8.22	11.57

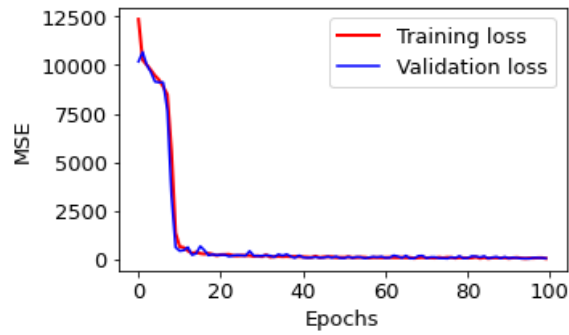


Fig. 4. Mean square error for training and validation for proposed 1-D CNN architecture.

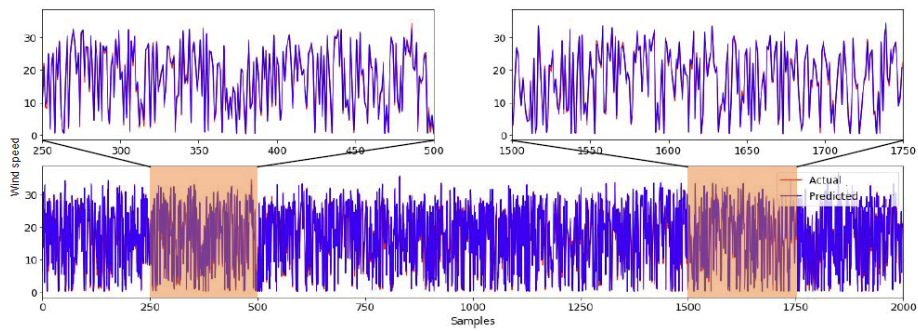


Fig. 5. Visualization of estimated wind field using the proposed method with respect to actual power for the randomly selected samples.

5 Conclusions

For an aircraft for several applications it is required to estimate wind-field dynamically during the mission. Wind-field estimate depends upon several variable like, trim conditions like airspeed, flight path angle and control inputs like aileron deflection, elevator deflection, rudder deflection and throttle input. Also, during a flight aircraft states change frequently due to different maneuvers and wind conditions. Due to dependence on many variables and their dynamic nature it requires enormous computational power to estimate wind-field dynamically. In this study, 1-D CNN has been designed to estimate the wind-field for an aircraft during the flight which is essential contribution of this study. Using the proposed method, the estimation of wind-field is faster and less complex than the conventional analytical approach and it can be applied to any aircraft. Also, this method does not require any additional hardware which makes it suitable for small and medium UAVs where weight and cost are critical. Estimation of wind-field using proposed method has also been verified for simulated results. Wind-field estimation model considers aircraft trim state that is easily available from autopilot as well as values of control inputs that are readily available.

The study presented in this paper is data-driven and the efforts we made to generate a comprehensive dataset through simulation. This approach indeed helps address the challenges of acquiring real-world data under varied wind conditions, which is essential for the robustness of our model. However, simulation provides a controlled environment, real-world testing is essential for validating our model's effectiveness. We plan to conduct practical flight tests in future work to gather empirical data and further refine our model based on those findings. Real-time testing can identify the shortcomings of the model's applicability and its feasibility for time-sensitive UAV operations. Further, the model is focused on trim flight conditions which may limit its applicability during dynamic maneuvers. In our future research, we aim to explore adaptive methods that can accommodate varying flight conditions and maneuvers, thereby enhancing the model's versatility in real-time applications.

Acknowledgments

This research was supported by the UKRI funded project Blueprint (project number 10025964).

References

1. The impact of wind on real world aircraft performance. www.corporatejetinvestor.com/news/how_wind_affects_aircraft_performance_625/ (Accessed : 2023 - 02 - 21)
2. Planes Could Save Serious Fuel Just by Riding the Wind. <https://www.popularmechanics.com/flight/airlines/a35393459/planes-could-save-fuel-by-riding-winds/> (Accessed: 2023-02-21)

3. Cheng, F., Gulding, J.: Computing Wind-Optimal Routes for Flight Performance Benchmarking. 16th AIAA Aviation Technology, Integration, and Operations Conference. doi = 10.2514/6.2016-4361 (2016)
4. Suzanne W. S., Phillip B. C., Adam L. H., Jamey D. J.: Catalyzing Collaboration for Multi-Disciplinary UAS Development with a Flight Campaign Focussed on Meteorology and Atmospheric Physics. AIAA Information Systems-AIAA Infotech @ Aerospace. 1156 (2016)
5. Jianghai Hu, Prandini, M., Sastry, S.: Aircraft conflict prediction in the presence of a spatially correlated wind field. IEEE Transactions on Intelligent Transportation Systems. 326-340(2005)
6. Wayman E. Baker, George D. Emmitt, Franklin R., Robert M. Atlas, John E. Molinari, David A. Bowdle, Jan Paegle, R. Michael Hardesty, Robert T. Menzies, T. N. Krishnamurti, Robert A. Brown, Madison J. Post, John R. Anderson, Andrew C. Lorenc, James McElroy: Lidar-Measured Winds from Space: A Key Component for Weather and Climate Prediction. Bulletin of the American Meteorological Society. 869 - 888 (1995)
7. United States. Flight Standards Service and United States. National Weather Service: Department of Transportation, Federal Aviation Administration, Flight Standards Service. Aviation Weather For Pilots and Flight Operations Personnel. (1975)
8. Moir, I., Seabridge, A.: Aircraft Systems: Mechanical, Electrical, and Avionics Subsystems Integration. AIAA education series (2011)
9. Cho, Am, Kim, Jihoon, Lee, Sanghyo, Kee, Changdon.: Wind Estimation and Airspeed Calibration using a UAV with a Single-Antenna GPS Receiver and Pitot Tube. IEEE Transactions on Aerospace and Electronic Systems. 109-117(2011)
10. Mekonen H. H., James L. G., Craig A. W.: Wind Estimation from an Unsteady Aerodynamic Aircraft Motion Model. AIAA SCITECH 2022 Forum. 0554 (2022)
11. Jingxuan, S., Boyang, L., Chih-Yung, W., Chih-Keng, C.: Model-Aided Wind Estimation Method for a Tail-Sitter Aircraft. IEEE Transactions on Aerospace and Electronic Systems. 1262-1278 (2020)
12. Seok-Woo, K., Han-Lim, C.: A Telemetry-Based Post-flight Wind Profile Estimation Method for Air-to-Surface Missiles. International Journal of Aeronautical and Space Sciences. 687-702(2021)
13. Velasco-Carrau, J., García-Nieto, S., Salcedo, J. V., Bishop, R. H.: Multi-Objective Optimization for Wind Estimation and Aircraft Model Identification. Journal of Guidance, Control, and Dynamics. 372-389 (2016)
14. Kenneth G., Jeremy W. H., Craig A. W.: Wind Estimation using an H-infinity Filter with Fixed-Wing Aircraft Flight Test Results. AIAA SCITECH 2023 Forum. 2252 (2023)
15. Dwivedi, V. S., Patrikar, J., Addamane, A., Ghosh, A. K.: MARAAL: A Low Altitude Long Endurance Solar Powered UAV For Surveillance and Mapping Applications. 2018 23rd International Conference on Methods Models in Automation Robotics (MMAR). 449-454(2018)
16. Raymer, D. P.: Aircraft Design: A conceptual approach. AIAA Education series, AIAA, Washington. (1992)
17. Lecun, Y., Bottou, L., Bengio, Y., Haffner, P.: Gradient-based learning applied to document recognition. Proceedings of the IEEE. 2278-2324 (1998)
18. Xiang, Z., Junbo, Z., Yann, L.: Character-level Convolutional Networks for Text Classification. Advances in Neural Information Processing Systems. Curran Associates, Inc. 28 (2015)